

## Ship-induced wave forces on a moored ship in the presence of uniform current

Hasan, Mohammad Saidee; Dastgheib, Ali; van der Hout, Arne; Roelvink, Dano

**DOI**

[10.1016/j.coastaleng.2025.104716](https://doi.org/10.1016/j.coastaleng.2025.104716)

**Publication date**

2025

**Document Version**

Final published version

**Published in**

Coastal Engineering

**Citation (APA)**

Hasan, M. S., Dastgheib, A., van der Hout, A., & Roelvink, D. (2025). Ship-induced wave forces on a moored ship in the presence of uniform current. *Coastal Engineering*, 198, Article 104716. <https://doi.org/10.1016/j.coastaleng.2025.104716>

**Important note**

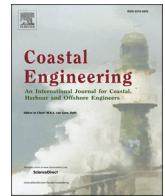
To cite this publication, please use the final published version (if applicable).  
Please check the document version above.

**Copyright**


Other than for strictly personal use, it is not permitted to download, forward or distribute the text or part of it, without the consent of the author(s) and/or copyright holder(s), unless the work is under an open content license such as Creative Commons.

**Takedown policy**

Please contact us and provide details if you believe this document breaches copyrights.  
We will remove access to the work immediately and investigate your claim.



# Ship-induced wave forces on a moored ship in the presence of uniform current

Mohammad Saidee Hasan<sup>a,b,e,\*</sup> , Ali Dastgheib<sup>b,d</sup>, Arne van der Hout<sup>a,c</sup>, Dano Roelvink<sup>a,b,c</sup>

<sup>a</sup> Delft University of Technology, Netherlands

<sup>b</sup> IHE Delft Institute for Water Education, Netherlands

<sup>c</sup> Deltares, Netherlands

<sup>d</sup> IMDC, Belgium

<sup>e</sup> Bangabandhu Sheikh Mujibur Rahman Maritime University, Bangladesh

## ARTICLE INFO

### Keywords:

Ship wave

Wave-ship interaction

Hydrodynamic loads

Moored ship

Non-hydrostatic model

XBeach

## ABSTRACT

Due to the increase in ship sizes and traffic, the effect of passing ships on the mooring forces of moored ships is becoming an increasingly more important aspect in restricted waterways, channels, and ports. The objective of the presented work is to investigate the effects of the presence of an ambient current on the hydrodynamic forces on moored ships when another vessel passes through the waterway.

In this research, XBeach-NH in (nonhq3d) mode is used to simulate passing ship effects, corresponding to test conditions as measured in physical model tests carried out at Deltares as a part of the JIP Ropes (Joint Industry Project, Research on Passing Effects on Ships) project (van der Hout and de Jong, 2014). Even though various layouts were tested in the Ropes project; the current paper focuses on the straight channel layout with different combinations of ship velocity and ambient current speed. Results show that XBeach slightly overestimates the draw down effects (water level depression) due to the primary waves, as well as the surge forces. And, the differences in surge forces between XBeach and measurement increases with increasing Froude number. However, sway forces and yaw moments are in better agreement with the measured data, even for higher Froude numbers, though slightly underestimated. This variation in results is consistent in almost all XBeach simulations. Results also indicate that ship velocities relative through water are more important than ship speed over ground in the presence of uniform current. However, in modelling exercises, it is advisable to run simulations implementing actual currents rather than simply adding or subtracting the current velocity to/from ship speed over ground to obtain a representative relative vessel through water, since in the latter case the duration of hydrodynamic force excitation on the moored vessel will not be realistic. Furthermore, simulations show that by only representing the correct relative speed through water in the simulations (and not the correct speed over ground), the surge force & yaw moment magnitude are underestimated in case of counter currents and sway forces are underestimated in case of following currents.

## 1. Introduction

The number of ports and ships that call on them has both increased over the years. Also, the size of the ships has gone up. According to an analysis (Hoffmann and Hoffmann, 2021) of data from 2005 to 2020, the size of the largest ship in the majority of the ports has increased. With this increase in ship size and the more frequent movement of ships, the number of marine accidents within port and harbour area has also got higher (Huang et al., 2019). Accidents may create delay in transportation by slowing down (un)loading processes or by causing channel

blockage and sometimes, though not common, leads to loss of valuable life. This emphasises the necessity of more efficient, innovative and safer design of the ports. To achieve this, several scientific challenges need to be addressed. Among others understanding the hydrodynamics and predicting the motion of the ships are of vital importance for safe passage, safe mooring, (un)loading operations, and to avoid marine accidents within the ports and harbours.

Even though commonly wind generated waves are the main contributor for ships and floating terminal motions, in sheltered water areas such as port basins, natural harbours, estuaries and navigation

\* Corresponding author: Delft University of Technology, Netherlands.

E-mail address: [m.s.hasan@tudelft.nl](mailto:m.s.hasan@tudelft.nl) (M.S. Hasan).

<https://doi.org/10.1016/j.coastaleng.2025.104716>

Received 26 November 2024; Received in revised form 10 January 2025; Accepted 27 January 2025

Available online 31 January 2025

0378-3839/© 2025 The Authors. Published by Elsevier B.V. This is an open access article under the CC BY license (<http://creativecommons.org/licenses/by/4.0/>).

channels, ship-generated waves may have significant impacts on nearby floating bodies in terms of motion and mooring loads (Zheng et al., 2023). Another phenomenon which can also cause significant motions of the ships moored in the harbour is harbour resonance (Kumar et al., 2016). When harbour resonance appears, long-period standing waves appear inside the harbour, accompanying with significant long-period oscillating current inside the harbour (Gao et al., 2023). In addition to harbour resonance, if the passing ship effect is also present it may even exacerbate the scenario hampering (un)loading operations of docks. Therefore, if the waves generated by passing ships can be simulated accurately, it will help to understand the consequences of it and what mitigation measure can be taken to prevent it. This will be beneficial for coastal and inland regions of the world where lots of ship are currently sailing or expected to sail due to future development of ports and harbours in those regions.

Earlier attempts to simulate hydrodynamic loads due to passing vessels employed linear numerical analysis using potential flow methods (Molen et al., 2010; Wang, 1975). However, shallow water effects which are nonlinear in nature, including interactions with nearby shorelines or complex geometries, cannot be represented (efficiently) with this tool. Hence, it is required to use available non-linear hydrodynamic time-domain models to predict passing ship effects. The double body method combining with the free surface method (to include free surface effects) was used by (Pinkster et al., 2004) for predicting these effects (hydrodynamic forces) of passing ship on a ship moored in harbour. Other coupled models e.g. coupling between 2DH time domain non-linear Boussinesq type wave model (TRITON) and 3D multibody panel method (DELMULTI) were also used to simulate wave-induced ship motion (Wenneker et al., 2006). In a study by (Dam et al., 2008), 2D depth-integrated Boussinesq equation was used to simulate the propagation of moving ship generated waves to determine the characteristics of ship waves in a narrow restricted channel (constrained by vertical walls).

Apart from numerical modelling, several physical model tests were carried out to assess passing ship effects. Kriebel conducted two different physical model test studies to determine the hydrodynamic loads on a moored ship due to forces imparted by a passing ship: for conditions where the passing vessel was parallel to the moored vessel in one study (Kriebel, 2007) and for conditions where the passing vessel is perpendicular to the moored vessel (Kriebel, 2010) in the other study. The time-histories of the surge force, sway force, and yaw moment were measured in both model tests. A new set of empirical equations were proposed by the authors for improved descriptions of the measured peak mooring loads. However, these were done in open boundary condition (without the presence of a quay). As mentioned in (Pinkster et al., 2004) the presence of the quay has significant impact on mooring force calculation compared to an open water conditions, increasing the surge force by about 80% and reducing the sway force and the yaw moment by about 60%. A recent study carried out in a physical model basin (Böttner and Kondziella, 2022) also found similar influences of quay walls. In their study, ships berthed at the quay experienced two to three times higher surge forces compared to open waters and the sway forces is reduced to approximately half of the ones at unrestricted condition in presence of quay walls. Therefore, the empirical equations are not suitable for conditions where a quay wall is present. Numerical or physical simulations may be more suitable alternatives for these conditions, especially in complex waterway geometries.

XBeach nonhydrostatic (XBeach-NH) with one or two layers (see section 3.3) has been used, together with the moving pressure field technique, to simulate the waves generated by the ship movement (Almström et al., 2021; de Jong et al., 2013; Ma, 2012). Those studies showed that this non-hydrostatic model can be used for estimating the waves generated by a passing ship and that it yields good results. However, fewer studies (Ai et al., 2023; Dam et al., 2008) are available on passing ship effects in the presence of current, which is a common situation, especially in regions where tidal or river flow exists and, it is

important to include ambient currents in passing ship wave analysis for those regions (Ai et al., 2023). All these studies were mostly concerned with calculating waves generated by passing ships (wave patterns) rather than the influence of these waves on nearby ships or other floating object motions. Only a few studies were carried out to calculate the mooring forces of the ships by extending the capabilities of XBeach-NH model (Zhou et al., 2015) and the results were not extensively validated against physical model tests or field measurements data. To do so, this paper investigates how well the XBeach-NH 2-layer numerical model can reproduce the results from physical model tests in the context of calculating forces on a moored ship due to a passing ship - with and without the presence of uniform current. And, with this advantage of including current, the XBeach-NH will allow for representing non-uniform bed levels/bathymetries as well as ambient currents in which moving vessels create waves that induce forces on moored vessels.

## 2. Passing ship effects on a moored ship

### 2.1. Ship generated waves

When a ship sails in water, the pressure near the bow increases as the vessel pushes the water around its bow yielding a rise in water level (bow wave), after that the pressure along the midship section decreases (drawdown) creating return current. Then the pressure again increases near the stern region of the ship creating stern waves as illustrated in Fig. 1. These waves are referred to as ship-generated waves and they propagate farther from the vessel.

The magnitude of this pressure variation depends on various factors e.g. vessel speed, draft and hull geometry. In shallow and restricted waterways, this pressure variation is also affected by water depth and cross-section of the waterway respectively.

In a channel or a river, the position of the passing ship relative to the quay wall or bank is an important parameter for ship-generated waves. When a ship sails through the centre line of channels or restricted waterways it induces a symmetric return current ( $U$ ) and when sailing eccentrically creates an asymmetric return current pattern. However, the discharge of the return current at both sides of the ship is about the same meaning the return current velocities, are larger between the ship and the nearest bank (Fig. 2), hence leading to a higher water level depression as well. This indicates that as the distance between the quay and the moving ship (passing distance) decreases, the water level depression in the quay side will increase in magnitude yielding higher passing ship effect.

Also, the higher velocity on one side creates a net force tending to push the ship to the bank of that side, and a moment tending to yaw the bow to the other side (far bank). This phenomenon is called bank suction (Van Koningsveld et al., 2021). A similar effect may occur when the ship is stationary, and instead of return current there is uniform flow (current) in the channel. Further discussion is provided in section 6.1.2.

### 2.2. Forces on the moored ship due to ship-generated waves

In Fig. 3 the general behaviour of the forces due to the passing ship is illustrated. The figure redrawn from (Kriebel, 2007) is based on the definition of forces used in this paper (Fig. 5). As the passing ship approaches, the moored ship experiences surge forces opposite to the sailing direction of the passing ship and sway forces towards the passing ship (negative force in our case), and a negative yaw moment. When the two ships are abreast ( $x/L = 0$ ) surge forces and yaw moments are near zero, while sway forces are maximum, i.e. the moored ship is pulled in toward the passing ship with maximum magnitude. Here,  $x$  is the centre-to-centre distance between moored and passing ship as shown in Fig. 3 and  $L$  is the length of the passing ship. As the ships cross, surge force switches to the opposite direction (positive force), sway force switches to positive (moored ship pushed towards the jetty), and yaw

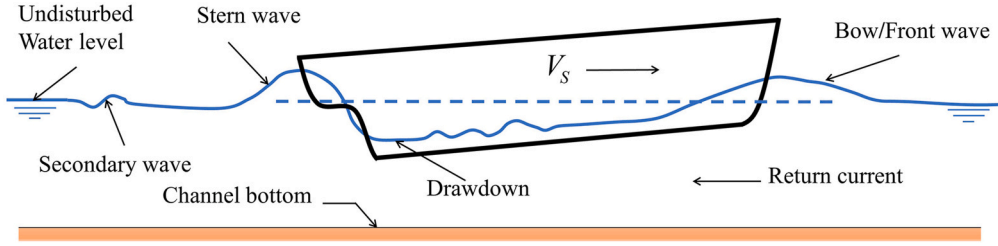


Fig. 1. Waves and return current due to ship movement in shallow restricted waterways (Redrawn from (Van Koningsveld et al., 2021)).

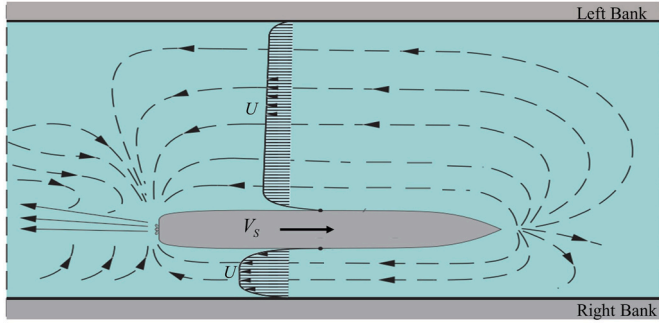


Fig. 2. Current pattern induced by sailing eccentrically (Van Koningsveld et al., 2021).

moment switches to positive.

### 2.3. Influence of current on loads due to passing ship effect

When current is present in the waterway, the ship velocities have to be considered relative to the current velocity in the undisturbed channel (Flory, 2002). Then the relative ship's velocity,  $V_{rel}$  can be calculated from the following equation, where  $V_c$  values is negative for counter current.

$$V_{rel} = V_s - V_c$$

Later in this paper in section 6.2.2, it will be checked whether simulating with this relative ship velocity by simply adding or subtracting current velocities to the ship velocities over ground is enough to fully mimic the effects of current on moored ship force calculation or is it better to include actual current during simulation.

## 3. Passing ship effects simulation in non-hydrostatic flow model (XBeach)

### 3.1. Coordinate system

For the passing ship effect simulation, the global coordinate system is defined, as shown in Fig. 4. Front, back, left, and right in Fig. 4a are used to define the boundary conditions.

The definition and direction of forces and moment on the moored ship used in this paper are illustrated in Fig. 5 and they are corresponded to the ship's local axis system. Surge force acts in the ship's x-axis and is positive towards the bow while sway acts in the y-axis and is positive towards the port side. The Yaw moment is the rotational moment around the z-axis.

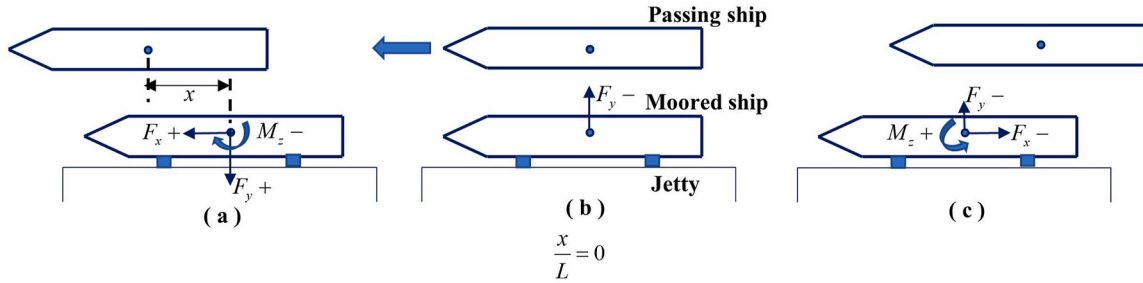


Fig. 3. Pattern of loads on moored ship as another vessel approaches (c), passes abeam (b), and departs (a) (Redrawn from Kriebel, 2007).

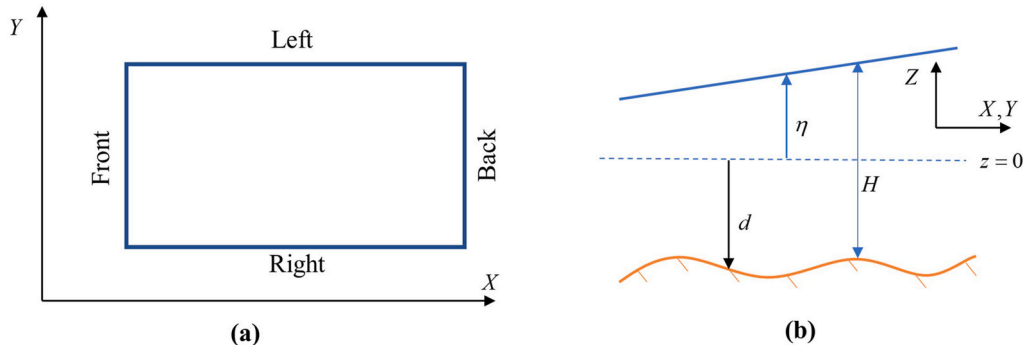


Fig. 4. Global coordinate system in XBeach; Horizontal (a) and Vertical (b).



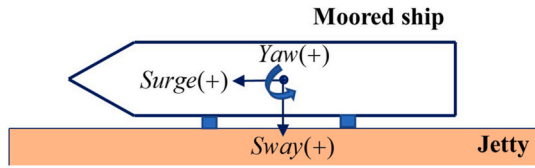


Fig. 5. Definition of forces and moment on the moored ship.

### 3.2. Generation of uniform flow (current) in XBeach

Uniform flow (current) in XBeach is generated using the flow boundary conditions and time-varying tide or discharge time series input. Vertically the domain is bound by the single-valued free surface  $z = \eta(x, t)$  and the bottom  $z = -d(x, t)$  as illustrated in Fig. 4b. At the boundary, the free surface elevation and depth-averaged velocity are the summation of the incoming (in) and reflected (out) signals as given in eq. (1).

$$\begin{aligned} u &= \bar{u} + u_{in} + u_{out} \\ z_s &= \bar{z}_s + z_{s,in} + z_{s,out} \end{aligned} \quad (1)$$

Where,  $\bar{u}$  = mean current velocity

$\bar{z}_s$  = mean free surface level

$u_{in}$  = incoming flow velocity

$z_{s,in}$  = incoming water level

$u_{out}$  = reflected flow velocity

$z_{s,out}$  = reflected water level

$u$  = flow velocity.

$z_s$  = water level

And, the incoming and outflow velocity is calculated from eq. (2).

$$\begin{aligned} u_{in} &= z_{s,in} \sqrt{\frac{g}{H}} \\ u_{out} &= -z_{s,out} \sqrt{\frac{g}{H}} \end{aligned} \quad (2)$$

Where,  $H$  = water depth as shown in Fig. 4.

From eqs. (1) and (2) we can derive eq. (3) for the calculation of flow velocity ( $u$ ) at the boundary,

$$u = 2u_{in} - \sqrt{\frac{g}{H}}(z_s - \bar{z}_s) + \bar{u} \quad (3)$$

The bed friction associated with mean currents is included via the formulation of the bed shear stress ( $\tau_b$ ) using the approach of (Ruessink et al., 2001) and both Chezy and Manning value can be used to determine the dimensionless bed friction coefficient ( $c_f$ ). In case of Chezy value ( $C$ ), the  $c_f$  value can be calculated from eq. (4) and in the Manning formulation the Manning coefficient ( $n$ ) must be specified and  $c_f$  is calculated from eq. (5).

$$c_f = \frac{g}{C^2} \quad (4)$$

$$c_f = \frac{gn^2}{h^{1/3}} \quad (5)$$

### 3.3. Propagation of ship waves in XBeach

In this work, the XBeach software is used to predict the passing ships effect. Several studies (de Jong et al., 2013; Zhou et al., 2013, 2015) showed non-hydrostatic model of Xbeach, together with the moving pressure field technique, can be implemented for estimating the waves generated by passing ships and they yield acceptable results. In the non-hydrostatic model, non-linear shallow water equations are solved along with a pressure correction term to model the propagation and decay of individual waves (Deltares, 2015). The non-hydrostatic mode

can be used by either one layer and the very recent development of the two-layer method. The mathematical formulation of the non-hydrostatic 1-layer model and numerical procedure of solving the equations in XBeach are well described in (Zhou et al., 2015). The 2-layer mode of XBeach (de Ridder et al., 2021) is a quasi-3D approach. The additional layer improves the frequency dispersion compared to the depth-averaged formulation without increasing additional computational costs (de Ridder et al., 2021). Making a comparison with linear wave theory it is found that the two-layer model can be applied until a  $k \cdot d$  of 4 (here,  $k$  is wave number and  $d$  is water depth), (de Ridder et al., 2021), which is higher than the one-layer model which is applicable till a  $k \cdot d$  of 2.5 (Roelvink et al., 2018). This allows us to further extend the capabilities of XBeach to simulate waves in relatively larger water depths (higher  $k \cdot d$  values) extending towards the intermediate water region.

### 3.4. Forcing of ship waves due to moving pressure field

As the passing ship moves through the computational domain, the water pressure head in each grid cell is interpolated from the ship grid onto the computational grid while maintaining the hull volume, see e.g. (Almström et al., 2021). This movement of the pressure field creates the ship-generated waves propagating in the computational domain and changes the water level where the other ship(s) is moored. The moored ship(s) is defined in the same way as the moving ship except it remains in the same position in the computational domain.

### 3.5. Computation of forces on a moored ship in XBeach

To compute the forces and moments on moored ships due to passing ships, the pressure head at each point on the 2-D grid defining the hull of the moored vessel (ship grid) is computed by interpolating the virtual water levels from the XBeach grid. Equations and brief descriptions of the interpolations between global and local grids can be found in (Almström et al., 2021). The virtual water levels are defined as the water levels at the ship locations (having effects of moving ship) plus the imposed pressure head (due to the moored ship itself) to the ship grid. Therefore, the pressure head ( $p_h$ ) at the ship hull is then computed by subtracting the undisturbed vertical position of the hull ( $z_{hull}$ ) from the virtual water level ( $z_s$ ) as illustrated in Fig. 6.

$$p_h = z_s - z_{hull} \quad (6)$$

For each grid cell on the hull the horizontal and vertical forces are then computed, and the total forces  $\vec{F}$  and moments  $\vec{M}$  are computed by integrating the pressure head over all cells (submerged surface,  $S$  of ship) and multiplying by water density,  $\rho$  and gravity,  $g$ .

$$\vec{F} = \rho \cdot g \cdot \iint_S p_h \cdot \vec{n} \cdot dS$$

$$\vec{M} = \rho \cdot g \cdot \iint_S p_h \cdot (\vec{r} \cdot \vec{n}) \cdot dS$$

in which  $\vec{n}$  is the outward normal vector on surface  $dS$  relative to the

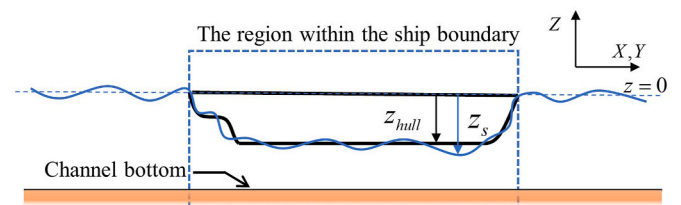


Fig. 6. Pressure head at the ship hull due to ship waves.

ship grid-cell surface and  $\vec{r}$  is the position vector of surface  $dS$  in the (x; y; z) coordinate system.

#### 4. Case study

For the case study physical model tests carried out at the Atlantic basin of Deltares are selected. The overview of the basin and the tests carried out are described by van der Hout and de Jong (2014). The passing ship in the model tests is the model of a Post-Panamax container vessel and the moored ship is a model of a Panamax container vessel. Full-scale properties of both ships are given in Table 1. Tests were carried out on a model scale of 1:100.

During the model tests, 7 different layouts were used, but for the present study, only the results from layout 1 are used as depicted in Fig. 7.

In layout 1, a straight channel having 18 m depth is used where the moored ship is parallel to the channel. In this straight channel layout, 20 different tests were carried out for two different passing distances ( $PD$ ), three different vessel speeds  $V_s$ , and five different current conditions. From the physical model tests different cases, as given in Table 2, are selected for investigation of the effects of both counter (opposite) current meaning flow velocity direction is opposite of passing ship velocity (sign of  $V_c$  is negative) and following current meaning flow velocity direction is same as passing ship velocity (sign of  $V_c$  is positive) using the non-hydrostatic flow model XBeach. All considered tests have the same  $PD$  of 107 m which is 2.5 times of the beam of the passing ship. This passing distance is shorter than the passing distance of 150 m which was available in the considered dataset. And, only tests with the smallest passing distance were selected for comparison, as the largest hydrodynamics loads on the moored ship are expected for this condition. Test 1.02 without current velocity is considered the *Base Case Scenario*. This test is conducted to get insights about the ship-generated wave effects when there is no current present in the simulation. The Relative Froude number in the table is defined as,  $Fr_{rel} = V_{rel}/\sqrt{gh}$  and it will be used during the result comparison between XBeach and measured data to check the variation of result for different  $Fr_{rel}$  range.

Apart from the case studies that are carried out to compare results with the results from physical model tests, additional case studies are carried out only in the XBeach with different combinations of relative velocity of ship ( $V_{rel}$ ) and ship speed over ground ( $V_s$ ) having various current conditions to get more insight in the effects of current magnitude and current direction.

#### 5. Numerical model set-up

##### 5.1. Bathymetry and ship depth file

The numerical model is prepared based on the properties of the channel and ship from the Deltares model test. As described in section 3.2 ships are represented by pressure heads depending on the draft of the ship in 2D representation. A separate grid (local ship grid) is used to define the ship by specifying the draft of the ship in each grid point as illustrated in Fig. 8. A ship track file is used to define the ship position for different time steps based on its speed and the pressure field in the global

grid cells is updated in each computational time step by interpolating the draft from the ship grid to the global grid, keeping the ship volume the same.

In Fig. 9 a snapshot (cropped) from the XBeach simulation is shown illustrating the moored and passing ship and the computed water level.

##### 5.2. Grid sensitivity

Before running all cases and scenarios, grid sensitivity tests were carried out and not much improvement was found reducing the overall computation global grid size than  $5 \times 5$  m. However, to capture the correct physical behaviour, the grid size was refined locally (around 1 m) in the y direction near the quay wall since the distance between the moored ship and the quay wall is around 3 m, less than one grid size (5 m). A grid size larger than the gap between the ship and the quay gives spurious initial sway force and yaw moments even before the passing ship approaches the moored ship. Therefore, this grid refinement as shown in Fig. 10 is an important aspect to be considered while calculating forces on moored ship near to a quay. And, the local ship grid needs to have a higher resolution than the global grid.

##### 5.3. Implementation of current

To use the method, mentioned in section 3.3 certain settings are implemented in the XBeach. For the channel boundary (as shown in Fig. 4a), a weakly reflective boundary condition is set in both the front and back of the channel. And, the left and right sides of the channel are defined as walls. There are two options in XBeach to implement current flow in the channel – tidal and discharge boundary conditions. The discharge boundary condition is relatively faster to achieve the desired flow velocity in the channel, hence used in our case. However, in previous versions of the XBeach, discharge boundary conditions can be defined as negative only meaning current flow can be implemented in one direction only. Small modifications allowed the mean current to flow in both directions while having weakly reflective boundaries. It helps to implement the following and opposing current in the channel for passing ship analysis by simply defining the discharge direction as negative or positive. And, Manning formulation was used to determine the dimensionless bed friction coefficient (cf) having a Manning coefficient ( $n$ ) of  $0.026 \text{ s/m}^{1/3}$ .

##### 5.4. Post-processing

A low pass filter was used to filter the XBeach results with a cut-off frequency of 0.033 Hz to filter out effects other than the primary waves. Filtered results are then compared against the Deltares physical model test results which were also filtered using same cut-off frequency from the raw data.

#### 6. Results and discussions

##### 6.1. Comparison of deltares measurements (DM) and XBeach results (XB)

###### 6.1.1. Base Case Scenario (without current)

Before comparing the effects of current, a base case simulation is carried out to get insights about the comparison of results when there is no current present in the simulation. In Fig. 11 water level changes at different point locations - (as given in Fig. 7) are plotted and in Fig. 12 forces and moment acting on the moored ship due to this water level change are plotted. In these figures results from Deltares measurements are indicated as (DM) and for XBeach results as (XB). From these two figures, we noticed that XBeach managed to get the correct pattern of the water level and forces even though there are differences in magnitude. Later in this section, a dimensionless results comparison is given to get more insight into the load pattern.

**Table 1**

Full scale properties of passing ship and moored ship.

Description	Passing ship	Moored ship
Length between perpendiculars	331.50 m	255.00 m
Length on Water line	337.75 m	261.00 m
Beam	42.90 m	32.26 m
Depth	23.00 m	25.00 m
Draft	14.50 m	12.00 m
Displacement (Actual)	127,037 m <sup>3</sup>	58,660 m <sup>3</sup>
Displacement (In XBeach)	125,469 m <sup>3</sup>	59,683 m <sup>3</sup>

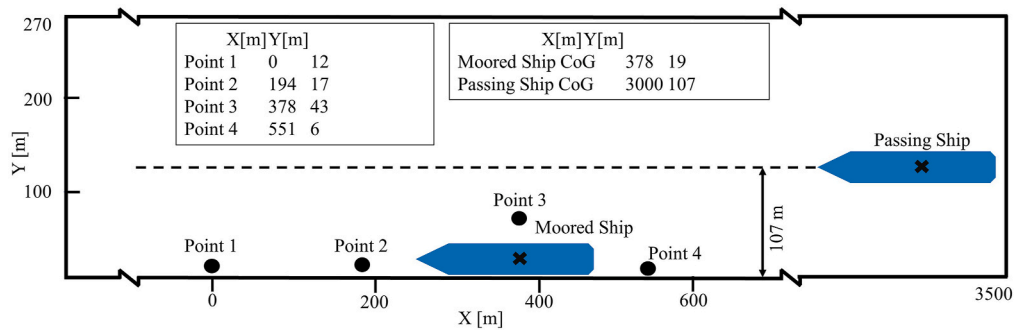


Fig. 7. Schematic layout of numerical model setup (prototype scale).

Table 2

Properties of selected test set-ups for case studies.

Test ID	Current dir.	Vs (kn)	Vc (kn)	Vrel (kn)	Fr <sub>rel</sub>
test1.01	Following	8.3	2.1	6.2	0.24
test1.02	–	8.3	0	8.3	0.32
test1.03	Counter	8.3	–1.5	9.8	0.38
test1.04	Counter	8.3	–1.9	10.2	0.39
test1.05	Counter	8.3	–2.8	11.1	0.43
test1.06	Following	10.4	2.1	8.3	0.32
test1.07	–	10.4	0	10.4	0.40
test1.08	Counter	10.4	–1.5	11.9	0.46
test1.09	Counter	10.4	–1.9	12.3	0.48
test1.10	Counter	10.4	–2.8	13.2	0.51
test1.12	–	12.5	0	12.5	0.48

Now, in terms of magnitude from Fig. 12, it is evident that XBeach overestimates the surge forces while it underestimates the sway and yaw. One reason behind this overestimation of surge forces is that the maximum water level drops (drawdown) calculated by XBeach is larger than the measurement value from the physical model tests (Fig. 11). Further research can be carried out to improve this estimation of

drawdown values, but it is not within the scope of this paper. This differences in results are also observed in other test cases without current (see Table 3 in appendices) and remain consistent in all cases meaning surge is overestimated whereas sway and yaw are underestimated in all cases. So, we expect to have this variation in results even when the current is implemented in the simulation.

To get more insights a dimensionless results comparison is carried out. Fig. 13 compares XBeach, measured results from physical model tests (van der Hout and de Jong, 2014), and idealized variation of loads from the theory of Wang (1975). The sway and yaw curves of Wang's theory are modified (multiplied by,  $-1$ ) to match the direction of XBeach results. Forces and moments from XBeach and measurements are divided by absolute maxima to get dimensionless form.

In Fig. 13, like Wang's theory for both the XBeach and measured data, the surge force and yaw moment have maxima (negative and positive) near at  $x/L = \pm 0.3$  and the maximum sway (negative maxima) is observed close to  $x/L = 0$ . This is similar to what was mentioned in section 2.2. In terms of magnitude, the dimensionless load pattern in the measurements and XBeach is almost similar; in Wang theory however, the forces and moments are symmetric with respect to  $x = 0$  axis. Wang's theoretical prediction indicates that surge force and yaw moment have

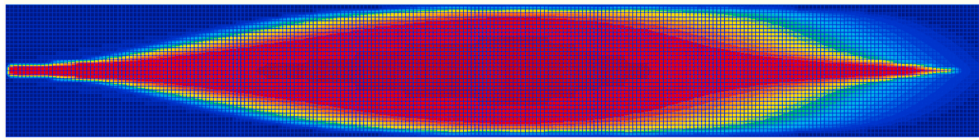


Fig. 8. 2D representation of a ship in local ship grid (colour represents ship draft in each grid). (For interpretation of the references to colour in this figure legend, the reader is referred to the Web version of this article.)

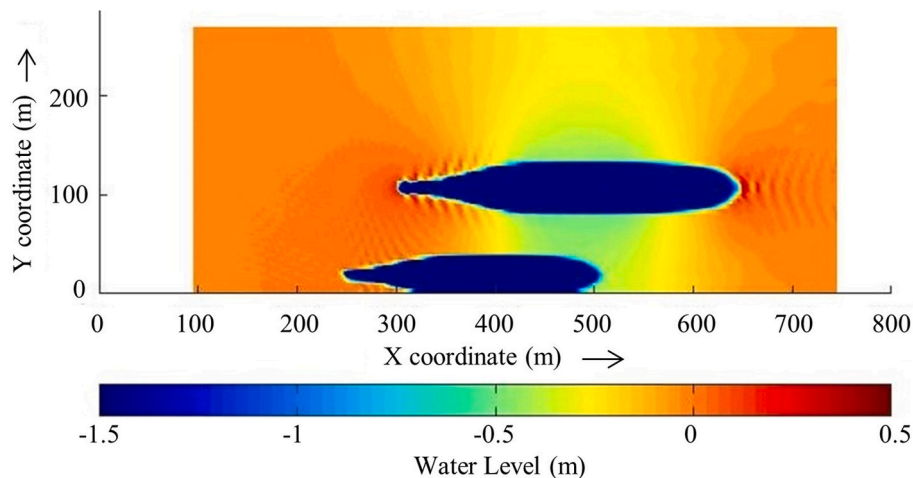


Fig. 9. Illustration of a passing ship simulation in XBeach (cropped).

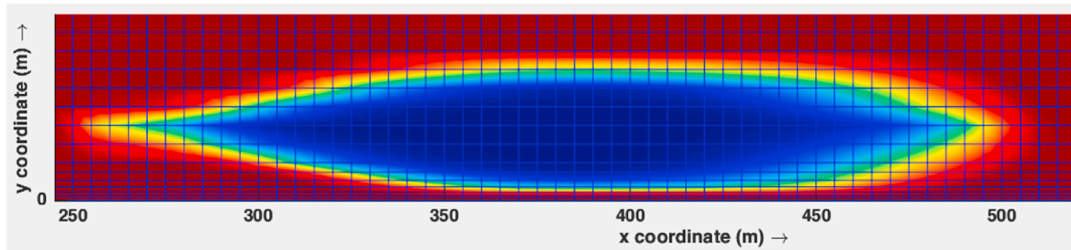


Fig. 10. Refinement of global grid near quay wall. Colours represent the draft of the vessel interpolated onto the global computational grid (from the local ship grid). (For interpretation of the references to colour in this figure legend, the reader is referred to the Web version of this article.)

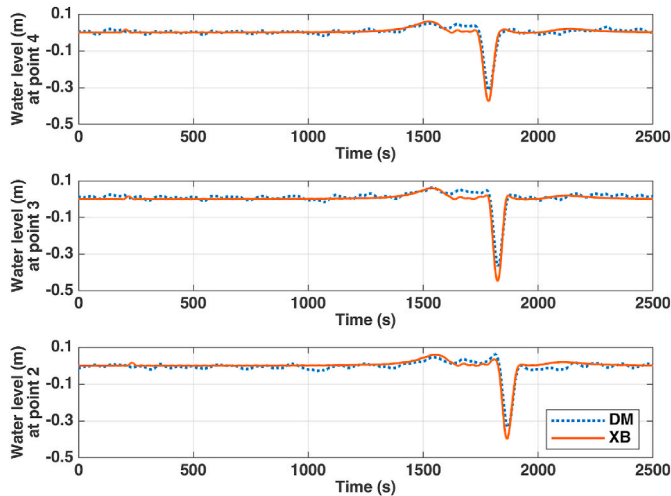


Fig. 11. Comparison of water levels (drawdown) with measured data for Ship speed 8.3 Knots (Test 1.02; see Table 2).

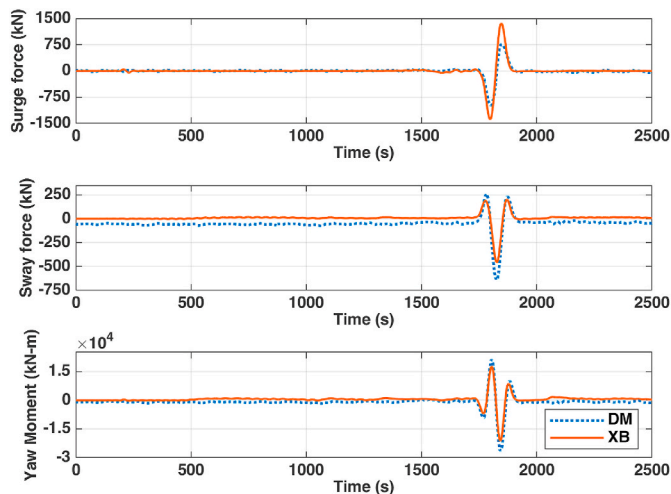


Fig. 12. Comparison of forces and moment with measured data for Ship speed 8.3 Knots (Test 1.02; see Table 2).

equal maxima in the positive and negative directions. However, measurement data and XBeach results in Fig. 13 show that the negative maxima of the surge is slightly larger than the positive maxima. The possible reason is that the Wang theory is based on potential flow theory.

Another observation is that the surge force starts increasing and reaches a peak due to the bow waves in the Wang theory, but in XBeach as well as in the measured data it is not present. Since Wang's theory is developed for open water conditions and only idealized variation (not

case specific) it is hard to conclude why this difference is observed. However, some 3D features of the ship e.g. bow, skeg, rudder etc are not accurately defined in the ship depth file of XBeach, therefore bow wave and stern wave of the ship may not be fully produced by the XBeach. To understand the capability of XBeach to produce these bow waves, further case studies having different ship hulls, with and without the bulbous bow, are needed to be carried out. Also, for ship-wave-induced forces on the moored ship, the effect of the bow wave is relatively small compared to the main drawdown effect of the primary wave.

#### 6.1.2. Static offset in load due to ambient current

In Figs. 14 and 15, the effect of the counter and following current is illustrated respectively, showing the measurement and XBeach results of tests 1.04 and test 1.01 (see Table 2). Without an ambient current, the external forces and moments on the moored vessel are zero until the waves generated by the passing vessel reach the moored ship. However, for the counter current case (Fig. 14) both the measured and XBeach results show a static offset compared to the condition without current (Fig. 12). The largest offset is visible in the Yaw moment, which has a negative value, with XBeach and the measured data showing almost the same magnitude. And, for surge and sway the magnitude is very low and not visible in Fig. 14.

For the following current (Fig. 15) the static offset for yaw is negative for both XBeach and measured data, but there is a significant difference in magnitude. In case of surge and sway similar magnitude of static offsets are visible in both XBeach and measured data. However, to check if this result is consistent, results from other test cases are also compared (Fig. 16).

In Fig. 16 static offset of various current conditions are plotted – in the 1st row for  $V_s$  8.3 knots (test 1.01 ~ test 1.05) and in the 2nd row for  $V_s$  10.4 knots (test 1.06 ~ test 1.10). Static offset is calculated by taking the average of values of 100 timesteps before the passing ship wave reaches the moored ship. Ideally, 1st and 2nd rows should give the same results. The reason is that even though the passing ship's actual velocity is different, the current conditions are the same. And passing ship velocity should not affect the static force offset acting on the moored ship since it only depends on the current flow velocity. In the case of XBeach results, we noticed that as well. However, in measured data from Deltares we see even though the current condition is the same the value of static offset is different. The reason could be that the test setups were not identical which is difficult to achieve in the physical set-up and there might be some effect from previous test runs or maybe some other reason. However, we have tried to compare results from measured data and XBeach to find some general trends.

In the left Fig. 16 (a & d) a small static offset in surge force can be seen, which increases in magnitude as the velocity of current increases. The sway force offset does not show any clear pattern in the case of measured data, but most cases give a positive offset. For the XBeach result, a slightly increasing trend is present for counter current as illustrated in the middle. Also, both the following and counter current give positive sway offset. The yaw offsets in XBeach are in good agreement with the measured data in case of counter current.

To summarise (see Fig. 17), when ambient current is present and a



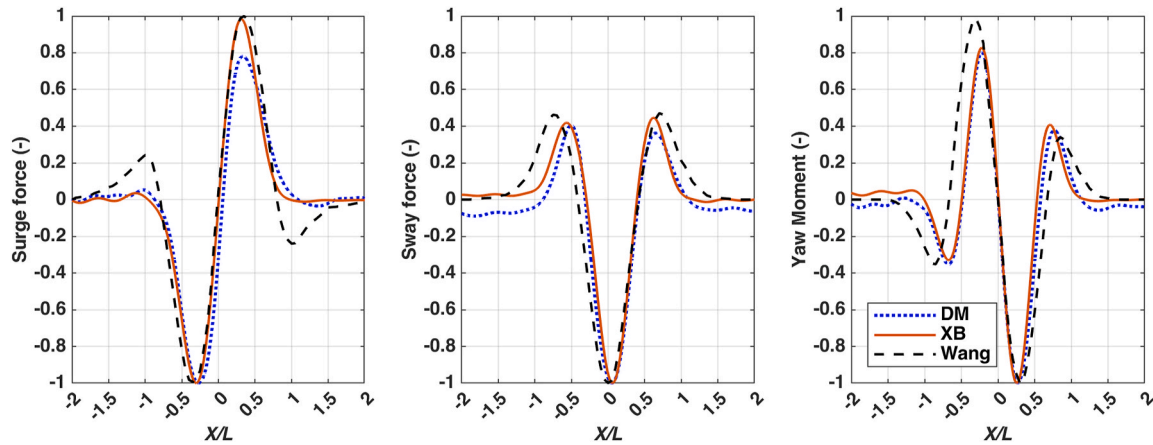


Fig. 13. Forces and moments on a moored vessel as a function of overtaking distance (here,  $L$  is the passing ship length and  $X$  is the centre-to-centre distance between ships).

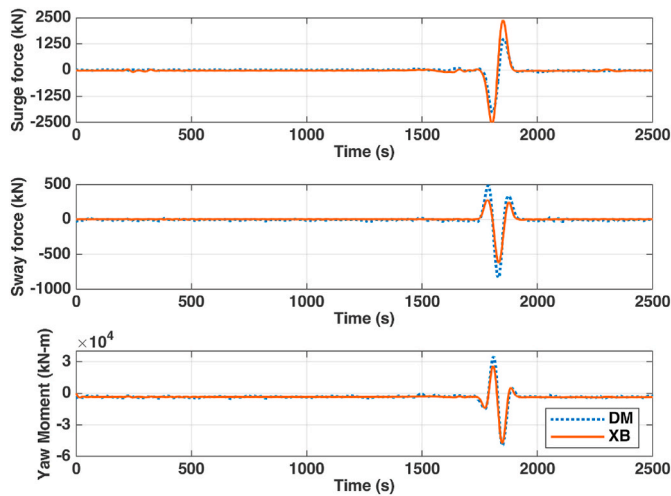


Fig. 14. Effects of counter current for a velocity of 1.9 knots opposite of passing ship sailing direction and ship speed of 8.3 knots (Test 1.04, see Table 2).

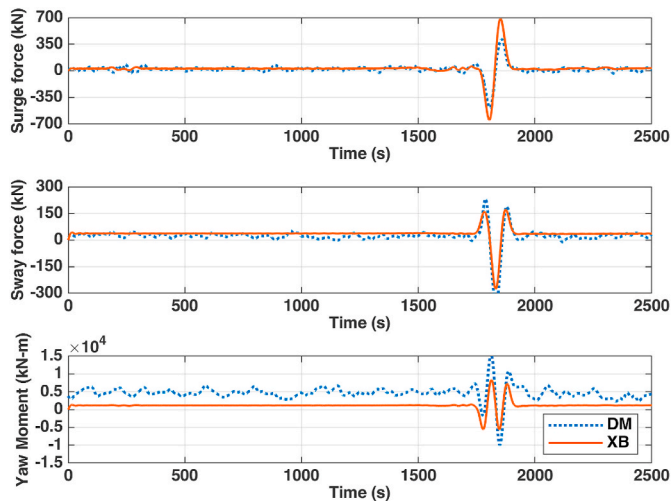


Fig. 15. Effects of the following current for a velocity of 2.1 knots in the sailing direction of passing ship and ship speed of 8.3 knots (Test 1.01, see Table 2).

ship is moored to the quay wall, the flow velocities, are higher between the ship and the quay wall since the discharge of the current at both sides of the moored ship is about the same. This means the pressure on the vessel side towards the quay is lower than on the other side of the vessel. This creates a similar effect to bank suction as described in section 2.1 and, therefore, causes a static force (sway) in the direction of the quay and a moment (yaw) pushing the bow off the quay and the stern towards the quay or vice versa depending on ship orientation w.r.t. current direction (Fig. 17). Due to the direct pressure of the current, a small static offset in surge force can also be found. And, it should be noted that the magnitude of all the static offsets may vary depending on the size and shape of the vessel even for the same uniform current velocity.

Even though these static offsets are much smaller than the excitation caused by the passing vessel which is evident in Figs. 14 and 15, it helps to check whether the current is implemented accurately in the simulation by observing the effect of it on the moored ship before the passing ship reached the moored ship. The current has a higher influence on the water-level drop around the sailing vessel (primary wave) since the magnitude of this water-level drop mainly depends on the velocity of the sailing ship relative to the water (van der Hout and de Jong, 2014). The influence of an ambient current is thus much more related to the change in primary wave height of the sailing vessel, resulting in large changes of wave exciting forces, than to the direct influence of the current on the moored ship.

### 6.1.3. Comparison of maximum and minimum

In Fig. 18, the maximum drawdown of water levels (max WL) for point 3 and point 4 (64 m and 101 m distance from passing ship centre of gravity respectively, see Fig. 7) are plotted against relative Froude number (Table 2). In general, both XBeach and measured data for points 3 and 4 show an increasing trend line as the  $Fr_{rel}$  increases. And, for all cases, max WL at point 3 is higher than point 4 since its distance from the passing ship centre of gravity is smaller. The differences between the Xbeach and measured results increase as the relative froude number (or relative ship velocity) increases for both point 3 and point 4. E.g., near  $Fr_{rel}$  of 0.25, the difference is around or less than 15 percent, whereas near  $Fr_{rel}$  of 0.50, the difference is around 50 percent, which is quite high.

In Fig. 19, the maximum absolute surge forces, sway forces and yaw moments are plotted for different test conditions against the relative Froude number, and the exact values are given in Appendix A. In the table, the negative sign indicates that the negative maximums are higher than the positive maximums which were also illustrated in Fig. 12 earlier. In general, from Fig. 19, it is evident that XBeach overestimates the surge forces and underestimates the sway forces and yaw moments. From the table, as well as in Fig. 19, we can also find that as the relative

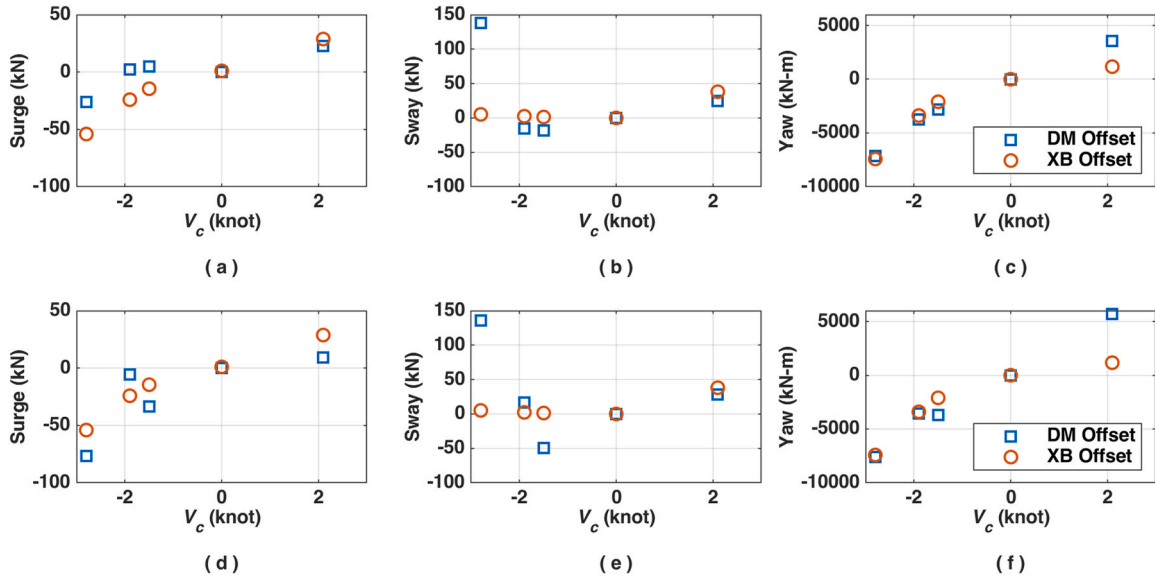


Fig. 16. Static offset of surge, sway and yaw due to different current velocities (in 1st-row test 1.01 ~ test 1.05 and in 2nd-row test 1.06 ~ test 1.10).

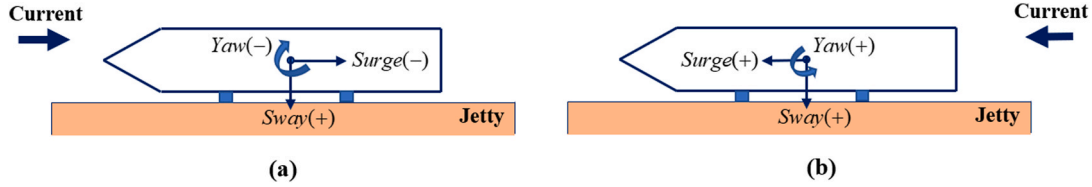


Fig. 17. Direction of static offset of surge, sway and yaw due to uniform current.

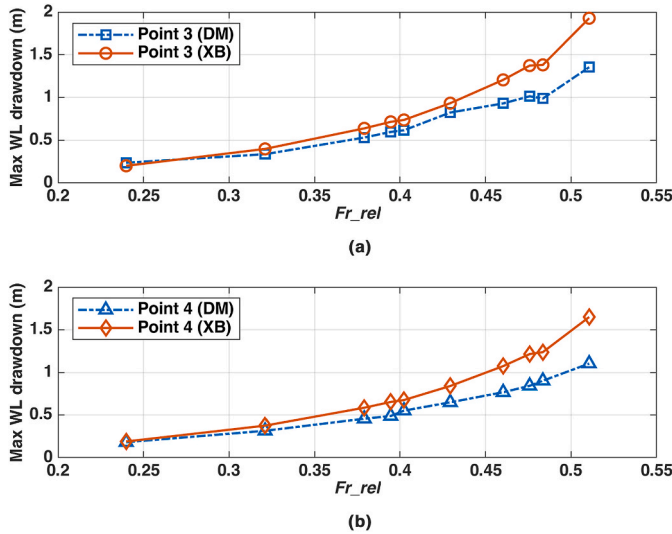


Fig. 18. Water levels for different combinations of ship and current velocities (test 1.01 ~ test 1.10).

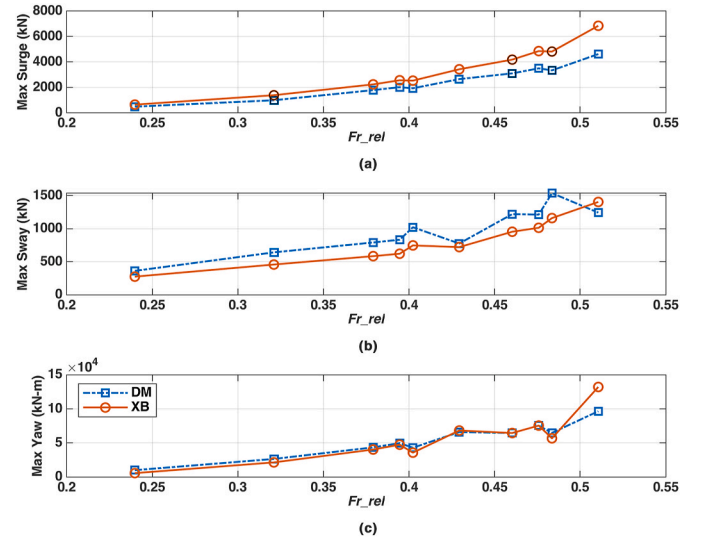


Fig. 19. Values of absolute maxima of surge, sway and yaw for different test conditions (test 1.01 ~ test 1.10).

Froude number increases the percentage differences in surge forces between XBeach and measured data increases. For sway the percentage difference is less than 30% for all cases and for yaw, it is less than 20%.

To understand only the effect of current, the ratio of absolute force maxima between conditions with and without current are plotted in Fig. 20 for both  $V_s = 8.3$  kn and  $V_s = 10.4$  kn for different current velocities. First, look at the ratios of counter current conditions ( $V_c$  sign is negative). As illustrated in these figures, for counter current surge force

ratios are in good agreement for XBeach and measured results for both  $V_s = 8.3$  kn (left column) and  $V_s = 10.4$  kn (right column). Even though from Fig. 19, we have noticed that as the  $Fr_{rel}$  increases the difference in absolute surge force maxima between XBeach and measured result also increases, we don't see a similar pattern for surge ratios rather they are in good agreement meaning relative current effects on surge forces compared to without current conditions are well simulated in XBeach. Sway ratios are also in good agreement except for high-velocity counter



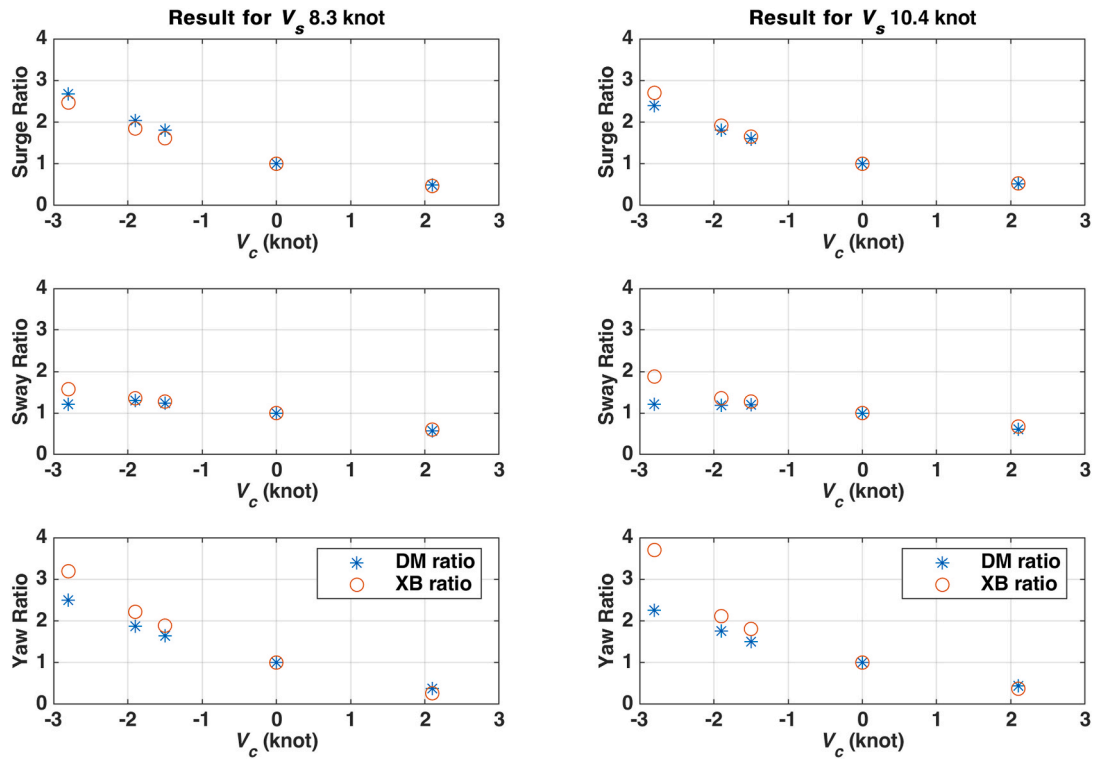


Fig. 20. Ratio of absolute maximum surge force, sway force and yaw moment for different current velocities concerning a condition without current for  $V_s = 8.3$  knots (left) and current for  $V_s = 10.4$  knots (right).

current  $V_c = -2.8$  kn. And, the yaw moment ratio increases as the counter current velocity increases, however, the differences are low for current velocity lower than 2 knots (meaning when the relative Froude number

$Fr_{rel}$  is lower than 0.5).

Now, for the following current condition, ratios for surge, sway and yaw are in good agreement for both  $V_s = 8.3$  kn &  $V_s = 10.4$  kn (Fig. 20).

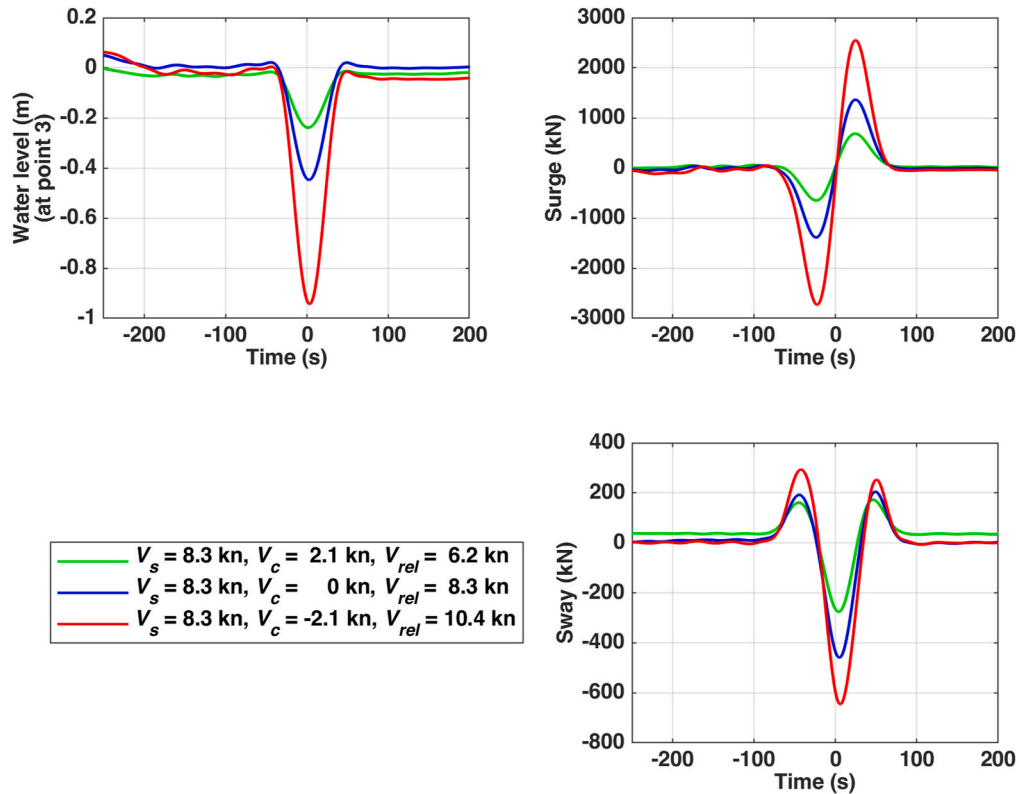


Fig. 21. Effects of current direction for a constant ship velocity ( $V_s = 8.3$  knots).

Therefore, we can conclude that even though the base case without current shows that there are differences in magnitude between measured forces and simulation results in XBeach (section 6.1), XBeach is capable of correctly simulating the effect of the current relative to without current condition when  $Fr_{rel}$  is lower than 0.5. later, we will look into some simulations carried out in XBeach within this  $Fr_{rel}$  range to understand more effects of current in case of passing ship events.

## 6.2. Analysis of XBeach results for different current velocities and directions

### 6.2.1. Influence of relative velocity of ship ( $V_{rel}$ ) and ship speed over ground ( $V_s$ )

As introduced in Section 4.1, different scenarios have been studied in XBeach. In Fig. 21, XBeach simulation results in which the vessel speed is kept constant, but the current magnitude and direction are varied (counter and following current) are shown.

From Fig. 21, it can be observed that the duration of the forces acting on the moored ship is the same in all simulations, indicating that the duration depends on the actual ship speed. However, in the case of magnitude of force as well as the water level drawdown there are differences in results. The drawdown of the water level for the counter current condition is more than double compared to no current condition and for the following current condition the effect is opposite (decreased by 50%). The reason behind this increase and decrease in water level is that the relative velocity of the ship w.r.t water ( $V_{rel}$ ) increases in case of counter current in contrast to following current. This water level differences also produce similar differences in surge forces – almost double and half for counter and following current respectively (Table 4). The sway force and yaw moments are also higher and lower respectively for counter and following current compared to the without current conditions (see Table 4 for actual values). This indicates that, in terms of magnitude, the relative velocity of the ship is more important than the actual ship velocity. Therefore, current velocity should always be considered while doing passing ship effect calculation when ambient current is present. That is why several authors (Flory, 2002; Seelig, 2001) used  $V_{rel}$  instead of  $V_s$  in their empirical formula to compute the passing ship effect. However, they simply subtracted the current velocity to achieve the required  $V_{rel}$  (described in section 2.3). In the next section the effect of using same  $V_{rel}$  will be discussed.

### 6.2.2. Influence of including actual current in the simulation

To check the applicability of methods which include current effect by simply subtracting current velocities from ship velocities, another scenario was created where relative velocities of ship,  $V_{rel}$  will be same, but with different ship velocities,  $V_s$  and current conditions.

In Fig. 22, even though in all cases the relative ship velocity,  $V_{rel}$  remains same, water level drop is higher in presence of counter current yielding a relatively higher surge forces (around 8% from Table 5) than the no current condition. However, in sway forces, we noticed the opposite scenario – here maximum sway force is higher (around 9% from Table 5) in the following current condition compared to no current condition. Also, since the actual velocity of the ship is lower in former case the surge force acts for longer time than in the other two cases. So, when simulation is carried out by simply adding or subtracting the

current velocity mentioned in the earlier section, it may underestimate the surge magnitude and duration in case of counter current condition and underestimate the sway forces in case of following current. To further check the relative magnitude of these differences in results, simulations are carried out in XBeach for different combination of  $V_s$  (8 knots  $\sim$  13 knots) and  $V_c$  (0.5 knots  $\sim$  3 knots).

In Figs. 23–25 surge forces, sway forces and yaw moments are plotted respectively for different combinations of  $V_s$  (8 knots  $\sim$  12.5 knots) and  $V_c$  (0.5 knots  $\sim$  3 knots). The upper panel (a) of these figures give the absolute force (or moment) maxima and the lower panel (b) gives the ratio of force (or moment) for conditions with current ( $V_{rel} = V_s - V_c$ ) divided by the force (or moment) without current for the same  $V_{rel}$  values ( $V_{rel} = V_s$ ). Therefore, points on line 1 which represent without current conditions ( $V_{rel} = V_s - 0$ ), when divided by the conditions at  $V_{rel} = V_s$ , give a value equal to 1. This line 1 is a reference line to compare the forces/moments when there is an opposing current, OP (line 2–4) and there is a following current, FO (line 5–7) present in the XBeach simulations.

Now, in case of Surge forces (Fig. 23) we can observe that as the opposing current velocity increases (line 2–4) the difference with no current also increases and this increase in differences follow similar pattern for all  $V_s$  (8–10 knots). And, for the following current (line 5–7) surge force ratio decreases meaning surge force is lower than without current conditions and this pattern is similar for all  $V_s$  (11–13 knots). However, these differences in results (even for the high current velocity of 3 knots) are within 10 percent for both OP and FO current conditions.

In case of sway (Fig. 24) we also notice differences in results for with and without current conditions. For opposing current sway forces are lower compared to no current conditions and for lower actual ship speed ( $V_s$ ) this difference is slightly higher (close to 20% for  $V_c = 3$  knots). When there is following current (line 5–7), sway forces are higher compared to no current conditions and the maximum difference is around 10%. The maximum differences in results are observed in the case of yaw moments (Fig. 25). Like surge yaw moments get higher as the value of opposing current increases and follow similar trend for all  $V_s$  value. However, the differences are quite high – even for current velocity of 1.5 knots the differences in results are more than 25% and for higher current velocities it goes beyond 50%. For following current differences in result ratio is lower compared to opposing current condition, however, they are still relatively high (around 50% for  $V_c$  of 3 knots).

In summary, while doing a simulation considering only  $V_{rel}$  and not actually including current in the simulation will overestimate the surge force & yaw moment for following current, and sway force for the opposing current. However, due to overestimation the results will be on the conservative side. But, surge force & yaw moment in opposing current and sway force for following current is higher than the without current conditions leading to underestimation of the actual forces and moment. Therefore, it is advisable to do the numerical simulation including the current when estimating current effects on forces of the moored ship due to passing ship especially for locations where sway force and yaw moment are significant since the differences in results for them are higher compared to surge force.

## 6.3. Limitations of the study

- We compared results for one following current condition,  $V_c = 2.1$  kn (in section 6.1.3) since in the physical model test only one following current condition was carried out. The reason why not more model tests have been carried out for following current conditions, was that with following current  $V_{rel}$  is even lower than  $V_s$  and for a relatively small  $V_{rel}$  the forces on the moored ship would be also relatively small (van der Hout and de Jong, 2014). Also, for lower  $V_{rel}$  (lower  $Fr_{rel}$ ) value XBeach and measurement results are in good agreement as seen in Fig. 19. Therefore, it does not have much impact on the results of the current study.

**Table 4**  
Maxima and minima of forces for scenario 1.

$V_s$ (kn)	$V_c$ (kn)	$V_{rel}$ (kn)	Surge Force (kN)		Sway Force (kN)		Yaw moment (kN-m)	
			Max	Min	Max	Min	Max	Min
8.3	2.1	6.2	686	−648	173	−276	8 387	−5 611
8.3	0	8.3		−1	205	−459	17687	−21365
			366	388				
8.3	−2.1	10.4	2	−2	293	−646	27238	−51464
			554	733				

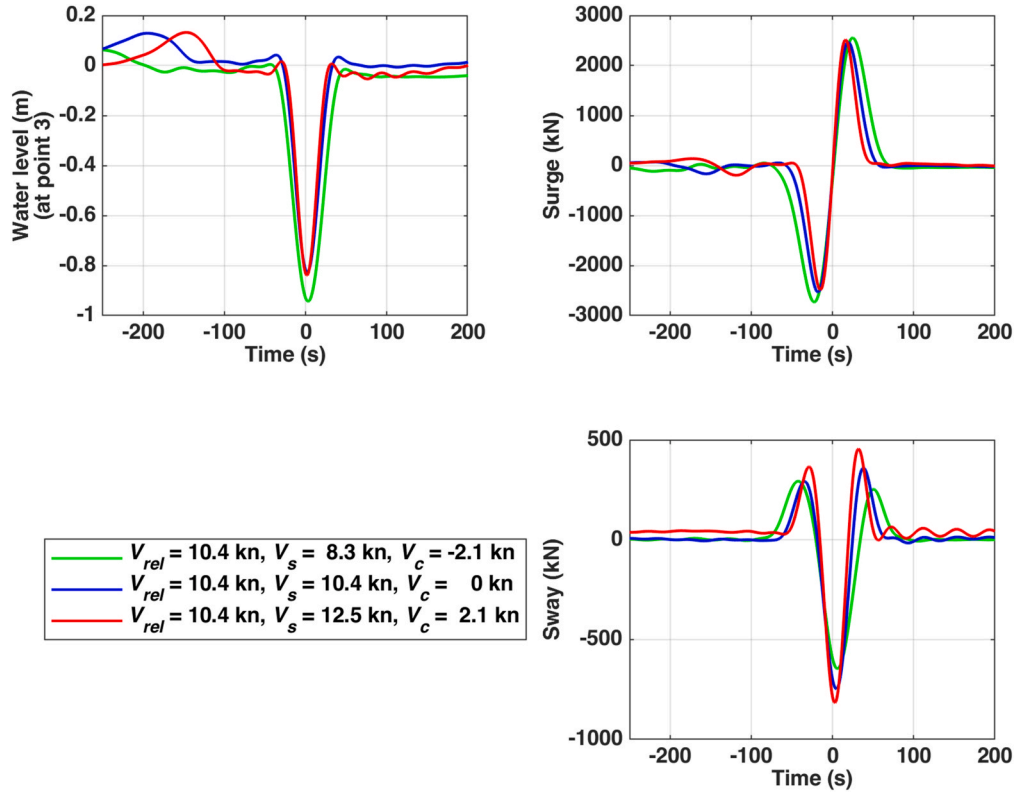


Fig. 22. Effects of relative velocity of ship w.r.t. to water for a constant ship relative velocity,  $V_{rel} = 10.4$  knots.

Table 5

Maxima and minima of forces for scenario 2.

$V_s$ (kn)	$V_c$ (kn)	$V_{rel}$ (kn)	Surge Force (kN)		Sway Force (kN)		Yaw moment (kN-m)	
8.3	-2.1	10.4	Max	Min	Max	Min	Max	Min
			2	-2	293	-646	27238	-51464
10.4	0	10.4	2	-2	360	-748	27456	-35688
			470	533				
12.5	2.1	10.4	2	-2	455	-817	25916	-24407
			518	487				

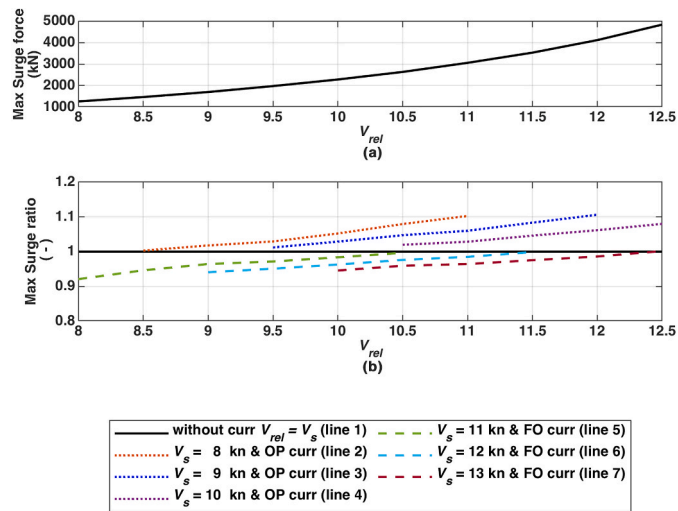


Fig. 23. Absolute surge force maxima (a) and relative max surge force (b) w.r.t conditions without current but same relative velocity ( $V_{rel} = V_s$ ).

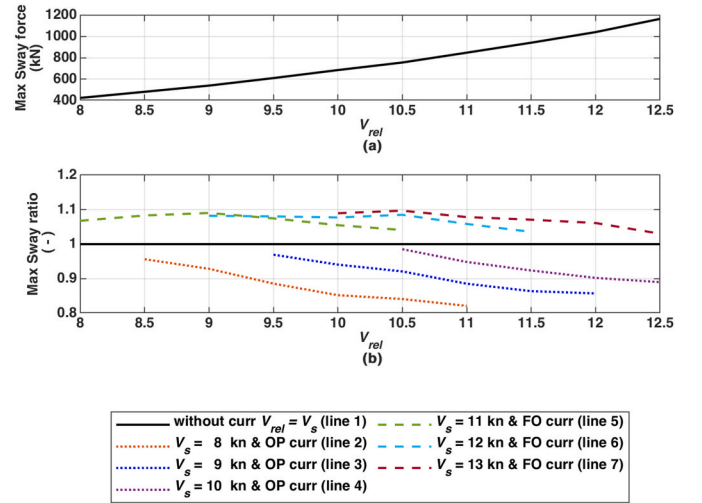


Fig. 24. Absolute sway force maxima (a) and relative max sway force (b) w.r.t conditions without current but same relative velocity ( $V_{rel} = V_s$ ).

b. As described in section 6.1.3, XBeach is capable of correctly simulating the effect of the current relative to without current condition when  $Fr_{rel}$  is lower than 0.5 ( $V_{rel}$  lower than 13 kn), hence simulations mentioned in section 6.2 were carried out within this range only. Further research/validation works need be carried out to check Xbeach capability beyond this  $Fr_{rel}$  (or  $V_{rel}$ ) range with different test set-ups e.g. different channel layout, ship dimensions, passing distance and ship speeds.

## 7. Conclusions

In this research work studies were carried out to check how well the

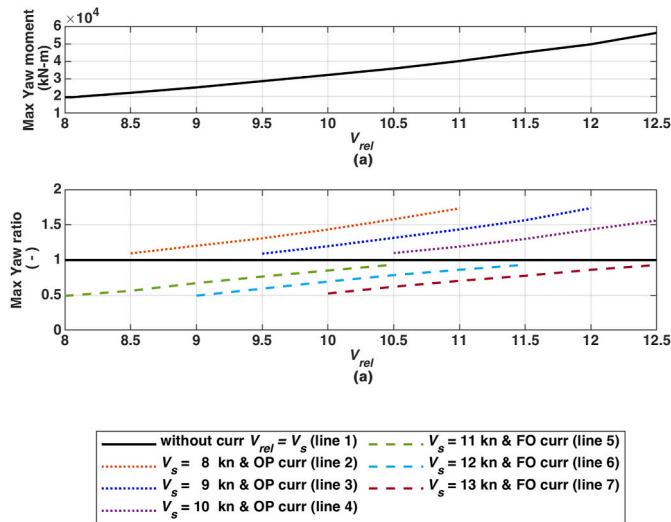


Fig. 25. Absolute yaw moment maxima (a) and relative max yaw moment (b) w.r.t conditions without current but same relative velocity ( $V_{rel} = V_s$ ).

XBeach can reproduce the results from a physical model test, especially in the presence of a uniform current. This research shows that XBeach slightly overestimates the drawdown effects (water level depression) due to the primary waves. Hence, the surge forces are also overestimated. And, sway forces and yaw moments are slightly underestimated compared to the measured data. However, this variation in results is consistent in almost all XBeach runs. Also, the ratio of absolute maximum values of surge, sway and yaw for different current velocities concerning zero currents value are in good agreement with measured data if the counter current velocity ( $V_c$ ) is lower than 3 kn and when  $Fr_{rel}$  is lower than 0.5.

From the analysis of the different scenarios it was found that, in presence of uniform current, the relative velocity is more important than

the actual ship velocity. However, even with the same relative ship velocity, differences in current magnitude and the direction current affect the magnitude of the surge force, sway force and yaw moment. And, unlike the magnitude of the forces, the duration of the forces acting on the moored ship depends only on the actual ship velocity, not the relative velocity. Furthermore, simulations should be carried out including actual current in the analysis and not by only representing the correct relative speed through water in the simulations (adjusting ship speed to account for current), for better estimation of the surge force, sway force and yaw moment magnitude.

#### CRediT authorship contribution statement

**Mohammad Saidee Hasan:** Writing – review & editing, Writing – original draft, Visualization, Validation, Resources, Methodology, Investigation, Funding acquisition, Formal analysis, Data curation, Conceptualization. **Ali Dastgheib:** Writing – review & editing, Supervision, Project administration, Methodology, Conceptualization. **Arne van der Hout:** Writing – review & editing, Supervision, Methodology, Conceptualization. **Dano Roelvink:** Writing – review & editing, Supervision, Software, Project administration, Methodology, Conceptualization.

#### Funding

The research project is supported by grant provided to Bangabandhu Sheikh Mujibur Rahman Maritime University, Bangladesh and IHE Delft Institute for Water Education by NUFFIC Netherland through Orange Knowledge Program (OKP).

#### Declaration of competing interest

The authors declare that they have no known competing financial interests or personal relationships that could have appeared to influence the work reported in this paper.

#### Appendices.

Table 3  
Values of maximum surge, sway and yaw for different test conditions

ID	$Fr_{rel}$	Surge (kN)			Sway (kN)			Yaw (kN-m)		
		XB	DM	% diff.	XB	DM	% diff.	XB	DM	% diff.
test1.01	0.24	-648	-489	32	-276	-364	-24	-5611	-9991	-44
test1.02	0.32	-1388	-992	40	-459	-588	-22	-21365	-26457	-19
test1.03	0.38	-2239	-1787	25	-586	-793	-26	-40300	-43447	-7
test1.04	0.39	-2562	-2019	27	-622	-834	-25	-47387	-49698	-5
test1.05	0.43	-3427	-2653	29	-723	-777	-7	-68190	-65963	3
test1.06	0.32	-1340	-1008	33	-505	-623	-19	-13294	-19156	-31
test1.07	0.40	-2533	-1932	31	-748	-1023	-27	-35688	-42858	-17
test1.08	0.46	-4185	-3104	35	-955	-1221	-22	-64503	-64523	0
test1.09	0.48	-4855	-3499	39	-1015	-1213	-16	-75444	-75401	0
test1.10	0.51	-6845	-4621	48	-1405	-1244	13	-132120	-96489	37
test1.12	0.48	-4818	-3340	44	-1161	-1539	-25	-56745	-64716	-12

#### Data availability

Data will be made available on request.

#### References

- Ai, C., Ma, Y., Sun, L., Dong, G., 2023. Numerical simulation of ship waves in the presence of a uniform current. *Coast. Eng.* 179, 104250. <https://doi.org/10.1016/j.coastaleng.2022.104250>.
- Almström, B., Roelvink, D., Larson, M., 2021. Predicting ship waves in sheltered waterways – an application of XBeach to the Stockholm Archipelago, Sweden. *Coast. Eng.* 170. <https://doi.org/10.1016/j.coastaleng.2021.104026>.

- Böttner, C.-U., Kondziella, B., 2022. Passing ship effect in shallow and confined waters, A systematic model test study of moored containership at quay. In: 6th MASHCON International Conference on Ship Manoeuvring in Shallow and Confined Water, with Special Focus on Port Manoeuvre. Glasgow.
- Dam, K.T., Tanimoto, K., Fatimah, E., 2008. Investigation of ship waves in a narrow channel. *J. Mar. Sci. Technol.* 13, 223–230. <https://doi.org/10.1007/s00773-008-0005-6>.
- de Jong, M.P.C., Roelvink, D., Reijmerink, S.P., Breederveld, C., 2013. Numerical modelling of passing-ship effects in complex geometries and on shallow water. *Smart Rivers* 95.1–95.7, 2013. <https://doi.org/10.13140/RG.2.1.1776.3049>.
- de Ridder, M.P., Smit, P.B., van Dongeren, A.R., McCall, R.T., Nederhoff, K., Reniers, A.J. H.M., 2021. Efficient two-layer non-hydrostatic wave model with accurate dispersive behaviour. *Coast. Eng.* 164, 103808. <https://doi.org/10.1016/j.coastaleng.2020.103808>.
- Deltares, 2015. XBeach Technical Reference: Kingsday Release.
- Flory, J.F., 2002. The effect of passing ships on moored ships. In: Prevention First 2002 Symposium, California State Lands Commission. Long Beach, CA.
- Gao, J., Shi, H., Zang, J., Liu, Y., 2023. Mechanism analysis on the mitigation of harbor resonance by periodic undulating topography. *Ocean Eng.* 281, 114923. <https://doi.org/10.1016/J.OCEANENG.2023.114923>.
- Hoffmann, Jan, Hoffmann, Julian, 2021. Bigger ships and fewer companies - two sides of the same coin | UNCTAD. Unctad 1–9.
- Kriebel, D., 2010. Mooring loads due to perpendicular passing ships. In: 12th Triannual International Conference on Ports. ASCE, Jacksonville, Florida. [https://doi.org/10.1061/41098\(368\)68](https://doi.org/10.1061/41098(368)68).
- Huang, D., Hu, H., Li, Y., 2019. Zero-Inflated Exponential Distribution of Casualty Rate in Ship Collision. *J. Shanghai Jiaotong Univ.* 24, 739–744. <https://doi.org/10.1007/s12204-019-2121-3>.
- Kriebel, D., 2007. Mooring loads due to parallel passing ships. In: 11th Triennial International Conference on Ports. ASCE, San Diego, California. [https://doi.org/10.1061/40834\(238\)46](https://doi.org/10.1061/40834(238)46).
- Kumar, P., Zhang, H., Ik Kim, K., Yuen, D.A., 2016. Modeling wave and spectral characteristics of moored ship motion in Pohang New Harbor under the resonance conditions. *Ocean Eng.* 119, 101–113. <https://doi.org/10.1016/J.OCEANENG.2016.04.027>.
- Ma, H., 2012. Passing Ship Effects in a 2DH Non-Hydrostatic Flow Model. IHE Delft Institute for Water Education.
- Molen, W. Van Der, Rossouw, M., Phelp, D., Tulsi, K., Terblanche, L., 2010. Innovative Technologies to Accurately Model Waves and Moored Ship Motions, vol. 2010. CSIR Third Bienn. Conf.
- Pinkster, J.A., Ruijter, M.N., Hydraulics, S., 2004. The Influence of Passing Ships on Ships Moored in Restricted Waters.
- Roelvink, D., McCall, R., Mehvar, S., Nederhoff, K., Dastgheib, A., 2018. Improving predictions of swash dynamics in XBeach: the role of groupiness and incident-band runup. *Coast. Eng.* 134, 103–123. <https://doi.org/10.1016/j.coastaleng.2017.07.004>.
- Ruessink, B.G., Miles, J.R., Feddersen, F., Guza, R.T., Elgar, S., 2001. Modeling the alongshore current on barred beaches. *J. Geophys. Res. Ocean.* 106, 22451–22463. <https://doi.org/10.1029/2000jc000766>.
- Seelig, W.N., 2001. Passing Ship Effects on Moored Ships. Washington, DC.
- van der Hout, A.J., de Jong, M.P.C., 2014. Passing Ship Effects in Complex Geometries and Currents, vol. 31. PIANC World Congr, p. 17.
- Van Koningsveld, M., Verheij, H.J., Taneja, P., De Vriend, H.J., 2021. Ports and Water Ways - Navigating the Changing World. TU Delft Open, Delft. <https://doi.org/10.5074/T.2021.004>.
- Wang, S., 1975. Dynamic effects of ship passage on moored vessels. *J. Waterw. Port, Coast. Ocean Eng. Harb. Coast. Div* 247–258.
- Wenneker, J., Borsboom, M., Pinkster, J.A., Weller, O., 2006. A Boussinesq-type wave model coupled to diffraction model to simulate wave-induced ship motion. In: Proceedings of the 31's PIANC Congress. Estoril, Portugal.
- Zheng, Z., Zou, L., Zou, Z., 2023. A numerical study on the effects of ship-generated waves on a moored ship in restricted waterways considering initial acceleration process. *J. Mar. Sci. Eng.* <https://doi.org/10.3390/jmse11030483>.
- Zhou, M., Roelvink, D., Verheij, H., Ligteringen, H., 2013. Study of passing ship effects along a bank. *Int. Work. Next gener. Naut. Traffic Model* 71–80.
- Zhou, M.G., Zou, Z.J., Roelvink, D., 2015. Prediction of ship-ship interactions in ports by a non-hydrostatic model. *J. Hydrodyn.* 27, 824–834. [https://doi.org/10.1016/S1001-6058\(15\)60545-5](https://doi.org/10.1016/S1001-6058(15)60545-5).